Peroxygenase-catalysed oxyfunctionalisation reactions

Hilberath, Thomas; Hollmann, Frank; Tieves, Florian; Zhang, Wuyuan

DOI
10.1016/bs.mie.2025.01.041

Publication date
2025

Document Version
Final published version

Published in
Biocatalysis Identifying novel enzymes and applying them in cell-free and whole-cell biocatalysis

CHAPTER TWENTY ONE

Peroxygenase-catalysed oxyfunctionalisation reactions

Thomas Hilberath[a], Frank Hollmann[a,*], Florian Tieves[b], and Wuyuan Zhang[c]

[a]Department of Biotechnology, Delft University of Technology, van der Maasweg 9, Delft, Netherlands
[b]Institute of Biochemistry, Heinrich Heine University Düsseldorf, Universitätsstraße 1, Düsseldorf, Germany
[c]Key Laboratory of Engineering Biology for Low-carbon Manufacturing, Tianjin Institute of Industrial Biotechnology, Chinese Academy of Sciences, 32 West 7th Avenue, Tianjin, P.R. China
*Corresponding author. e-mail address: f.hollmann@tudelft.nl

Contents

Abstract

Peroxygenases represent a class of versatile heme-thiolate enzymes capable of catalysing highly selective oxyfunctionalisation reactions, particularly the hydroxylation of non-activated C-H bonds. This transformation, which poses substantial challenges in conventional organic synthesis, underscores the potential of peroxygenases in green chemistry applications. While cytochrome P450 monooxygenases have long been the

Methods in Enzymology, Volume 714
ISSN 0076-6879, https://doi.org/10.1016/bs.mie.2025.01.041

primary focus for such biocatalytic transformations, their industrial adoption has been limited due to complex electron transfer chains and cofactor requirements. In contrast, peroxygenases bypass these limitations by directly utilising hydrogen peroxide (H_2O_2) to activate the catalytic heme site, thereby circumventing the oxygen dilemma typically encountered in P450 catalysis. Key milestones in peroxygenase research include the identification of chloroperoxidase from *Caldariomyces fumago* and the subsequent discovery of unspecific peroxygenases, such as those from *Agrocybe aegerita*, which exhibit broad substrate specificity and high catalytic efficiency. Here, we explore the mechanistic pathway of peroxygenase-catalysed reactions, emphasising the formation and decay of Compound I and the catalytic cycle's various functional outcomes. Critical aspects such as *in situ* H_2O_2 generation to mitigate enzyme inactivation, substrate loading strategies for practical applications, and the role of enzyme and reaction engineering in enhancing regio- and stereoselectivity are examined. Additionally, we address challenges in reaction scalability and operational stability for preparative-scale applications, offering insights into innovative protocols involving immobilised enzymes and non-aqueous reaction media. This review highlights recent advancements in the peroxygenase field and underscores the enzyme's promising role in sustainable oxyfunctionalisation reactions.

1. Introduction to peroxygenases

Peroxygenases (EC 1.11.2.1) are a group of heme-thiolate enzymes performing oxidation and oxyfunctionalisations that are of great importance for organic synthesis. Especially the selective hydroxylation of non-activated C-H bonds represents a transformation that is notoriously difficult for classical organic chemistry.

To address this issue, for a long time, cytochrome P450 monooxygenases have been in focus of biocatalysis research. However, after four decades of intensive research, the impact of P450 monooxygenases on organic synthesis, except for the pharma context, has been rather limited. Several factors may account for this. On the one hand, the complex electron transport chain and the dependency on costly cofactors but also costly stoichiometric cosubstrates may impede their broader application. On the other hand, also the so-called *Oxygen Dilemma* (Fig. 1) complicates P450-catalysed reactions on a preparative scale.

Peroxygenases share with P450 monooxygenases the prosthetic group (a heme cofactor attached to the enzyme via a cysteine as distal ligand). However, in contrast to the latter, peroxygenases efficiently use hydrogen peroxide and some organic hydroperoxides to form the catalytically active compound I (CpdI) (Fig. 1).

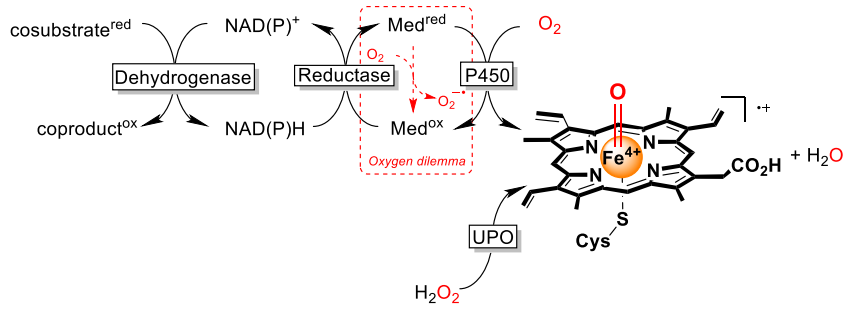

Fig. 1 Comparison of the Compound I-formation mechanisms of P450 monooxygenases and peroxygenases. The catalytic mechanism of P450 monooxygenases comprises the involvement of single electron transfers (SET) to the heme Fe-ion. These SET steps, however, are prone to direct electron transfer to dissolved O_2 resulting in superoxide (and eventually H_2O_2).

The first peroxygenase was reported by Hager and coworkers already in the 1960s (Morris & Hager, 1966) and subsequently received considerable interest as simple oxyfunctionalisation catalyst (van Rantwijk & Sheldon, 2000). Interestingly, this enzyme still today is most widely known as Chloroperoxidase (CPO, from *Caldariomyces fumago*, now *Leptoxyphium fumago*). Unfortunately, CPO turned out to be efficient (for a discussion on efficiency in the context of catalysis *vide infra*) as sulfoxidation catalyst whereas its performance on C-H bonds is somewhat disappointing (van Rantwijk & Sheldon, 2000).

The next milestone in peroxygenase catalysis was the discovery of the so-called unspecific peroxygenase from *Agrocybe aegerita* (*Aae*UPO) by Hofrichter and coworkers (Ullrich, Nüske, Scheibner, Spantzel, & Hofrichter, 2004). Interestingly again, this enzyme was first described as haloperoxidase even though its halide oxidation activity has receded into the background recently making place for a myriad of selective oxyfunctionalisation applications (Beltrán-Nogal et al., 2022; Hobisch et al., 2021; Monterrey, Menés-Rubio, Keser, Gonzalez-Perez, & Alcalde, 2023). The development of a recombinant expression system (Molina-Espeja, Ma, Mate, Ludwig, & Alcalde, 2015) and an engineering platform (Molina-Espeja et al., 2014; Molina-Espeja, De Santos, & Alcalde, 2017) by the Alcalde group enabled the spreading of *Aae*UPO to a wider community. Also based on these developments, the number of newly described peroxygenases from different origins is increasing rapidly in the past years (Beltrán-Nogal et al., 2022; Monterrey et al., 2023).

2. Mechanism of peroxygenases

The catalytic mechanism of peroxygenases basically comprises the so-called hydrogen peroxide shunt pathway known for P450 monooxygenases (Hrycay, Gustafsson, Ingelmansundberg, & Ernster, 1975). However, in contrast to the latter, peroxygenases exhibit much higher catalytic activity with H_2O_2.

In the first steps of the peroxygenase mechanism H_2O_2 binds to the resting state of the enzyme forming the so-called compound I (CpdI) in a sequence of deprotonation/reprotonation and water elimination. The acid-base pair Glu/Arg is believed to play a major role in these steps (Fig. 2). Once formed, CpdI can undergo various reactions. The classical hydroxylation mechanism comprises a hydrogen abstraction step from the bound starting material followed by rapid recombination of the Fe-bound OH group with the carbon radical. In case, the initial radical is relatively stable,

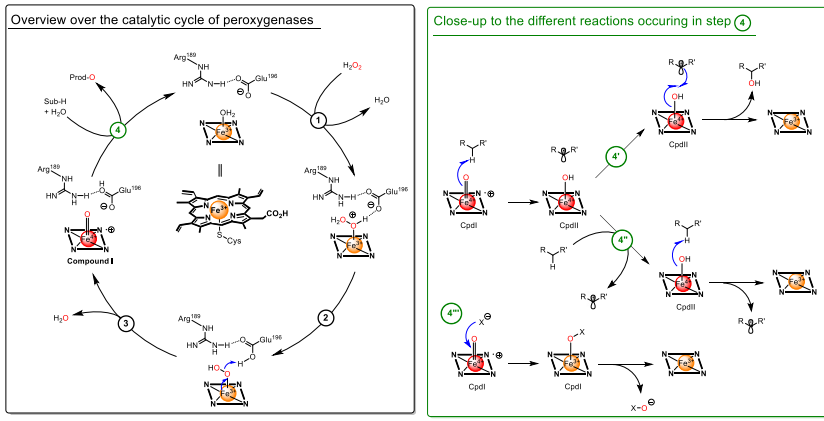

Fig. 2 Schematic representation of the peroxygenase mechanism. Left: Overall catalytic cycle with a focus on Compound I (CpdI) formation and right: the various reaction pathways for CpdI. Step 1: From the resting state, the catalytic cycle is initiated by replacement of the water ligand by H_2O_2. In steps 2 and 3, the primary adduct is deprotonated/re-protonated facilitating water elimination and formation of CpdI. In step 4, CpdI decays via substrate oxidation back into the resting state. Depending on the enzyme and/or substrate, step 4 can proceed via H-atom abstraction from a bound organic substrate. Depending on the stabilisation of the radical species formed, either a fast rebound of the Fe-coordinated OH to the radical yields an alcohol product (step 4′). In case of stabilised (conjugated) radicals with a higher life-time, the radical can also leave the enzyme active site making place for another substrate to be converted. This reaction yields two radical species per H_2O_2 equivalent. In the presence of halides, also a halide oxyfunctionalisation can occur (step 4″).

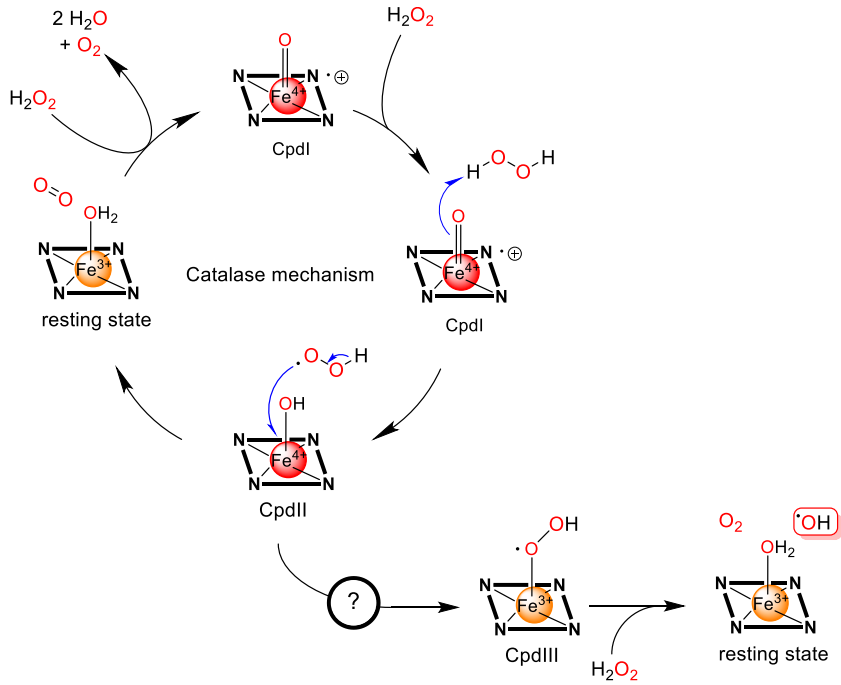

Fig. 3 Proposed inactivation mechanism of heme-containing enzymes by H_2O_2.

it also can leave the active site making space for another substrate molecule to be converted into a radical (peroxidase reaction). Some peroxidases also exhibit a haloperoxidase activity forming hypohalites. Finally, also the catalase activity of peroxygenases is worth mentioning (Fig. 3).

3. *In situ* H_2O_2 generation

Heme enzymes including peroxygenases are irreversibly inactivated by H_2O_2. Hofrichter and coworkers have proposed a malfunction of the catalase mechanism of peroxygenases to form hydroxyl radicals which eventually degrade the porphyrin moiety and thereby account for the irreversible inactivation (Fig. 3) (Karich, Scheibner, Ullrich, & Hofrichter, 2016). In essence, the catalase mechanism of heme enzymes comprises a hydrogen abstraction from an additional H_2O_2 molecule bound to CpdI. The resulting CpdII mostly decomposes into the resting state and O_2. Sometimes, however, it also can decompose into CpdIII which then liberates highly reactive hydroxyl radicals responsible for the heme degradation.

It has yet to be demonstrated whether this highly undesirable side reaction can be avoided or alleviated through protein engineering. However, a solution lies in reaction engineering. By maximising the reaction of CpdI with the desired substrate and minimising its reaction with H_2O_2, both the catalase activity and the harmful malfunction can be reduced. Therefore, controlling the *in situ* concentration of H_2O_2 can significantly improve the operational stability of peroxygenases. Two viable approaches to achieve this control are defined external addition of H_2O_2 or its *in situ* generation via the reduction of molecular oxygen.

External dosing of H_2O_2 is very straightforward but goes hand in hand with a continuous dilution of the reaction mixture, which may not always be desirable. This issue is circumvented by *in situ* H_2O_2 generation. This approach, however necessitates additional reducing equivalents for the reductive activation of O_2. Table 1 summarises a range of recent *in situ* H_2O_2 generation methods.

Additionally, supplying O_2 to the reaction medium can present a challenge. Achieving high productivity requires efficient O_2 delivery, but the phase transfer rate of O_2 from the gas phase quickly becomes a limiting factor (Anderson, Bommarius, Woodley, & Bommarius, 2021; Birmingham et al., 2021; Dias Gomes et al., 2019; Lindeque & Woodley, 2020). This issue is particularly critical in small-scale reactions (<10 mL), where careful attention is needed. The rate of shaking, stirring, or bubbling can not only affect the O_2 transfer rate but may also lead to enzyme inactivation and, in the case of volatile reagents, create issues with mass balance.

4. Increasing the substrate loading

Many, if not most substrates of interest are poorly soluble in water, which is why the majority of peroxygenase reactions is still performed with low (<10 mM) substrate concentrations (Wu, Paul, & Hollmann, 2024). While such conditions are certainly suitable for proof-of-concept studies, they are not sustainable both from an environmental nor economic perspective. Consequently, increasing the reactant loading is of utmost importance if preparative or even industrial applications are envisaged (Van Schie, Spöring, Bocola, Dominguez de Maria, & Rother, 2021).

One possibility is to use water-soluble cosolvents such as ethanol, acetone, acetonitrile, DMSO, etc. Particularly the peroxygenase variant

Table 1 Selected examples of *in situ* H_2O_2 generation systems used to promote peroxygenase-catalysed oxyfunctionalisations.

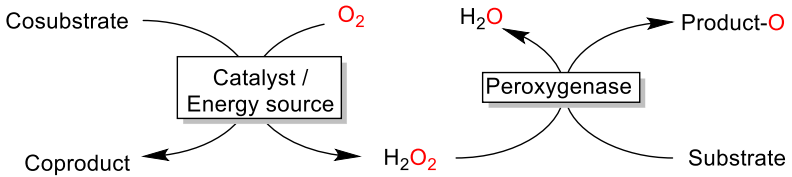

Cosubstrate	Coproduct	Catalyst/energy source	Waste [g mol^{-1}_{H2O2}]	Remarks/References
Glucose	Gluconolactone	GOx	178	Well-established, robust, large amounts of waste (Van De Velde Lourenço Bakker van Rantwijk & Sheldon, 2000)
Ethanol	Acetaldehyde	AOx	44	Problematic coproduct (But et al., 2017)
Formic acid	CO_2	FOx	44	Tieves et al. (2019a)
Methanol	CO_2	FOx	14.7	Willot et al. (2020)
Water	O_2	TiO_2 / hν	8	Experimental (Zhang et al., 2018)
—	—	Cathode	-[a]	Specialised equipment (Sayoga et al., 2023)

PaDa-I from *Agrocybe aegerita* has been shown to be remarkably resistant to such cosolvents (Hilberath, Van Troost, Alcalde, & Hollmann, 2022) and product concentrations of up to 300 mM have been achieved with this approach (Hilberath et al., 2023). It remains to be shown if this high solvent tolerance is unique for PaDa-I or a general feature of peroxygenases. Another issue to keep in mind when using water miscible cosolvents is their possible transformation by peroxygenases (e.g. alcohols are frequently oxidised to their carbonyl pendants) and possible difficulties in downstream processing (e.g. if the boiling points of the different components are too close and/or if azeotropes are being formed).

Another possibility is to make use of so-called multiphase reaction setups. Particularly popular are two-liquid phase-systems (2LPSs) in which a hydrophobic, water insoluble solvent serves as substrate reservoir and product sink. When deciding for such reaction systems, issues of interfacial inactivation of the biocatalyst(s), phase transfer rate limitations and also the undesired oxyfunctionalisation of the organic solvent have to be taken into account.

Finally, also non-aqueous reaction media are worth to be mentioned. Immobilised peroxidases have been shown as early as the 1980s by Klibanov and coworkers to operate under non-aqueous conditions (Dordick, Marletta, & Klibanov, 1986; Dordick, Marletta, & Klibanov, 1987; Zaks & Klibanov, 1984, 1985). It is important to note that aqueous H_2O_2 is not suitable for these conditions. Organic hydroperoxides represent a doable alternative (Shen et al., 2024).

5. Selectivity issues

Various selectivity issues can arise in peroxygenase-catalysed reactions. In particular, stereo- and regioselectivity challenges can generally be addressed through enzyme engineering (de Santos et al., 2023; Münch et al., 2023, 2024; Gomez de Santos et al., 2023). However, some issues can also be tackled through reaction engineering. For example, in arene hydroxylation, undesired peroxidase activity (Fig. 2) is observed. In this case, the phenol product formed undergoes further conversion into a phenoxy radical, which may subsequently undergo spontaneous oligo-/polymerisation (Fig. 4).

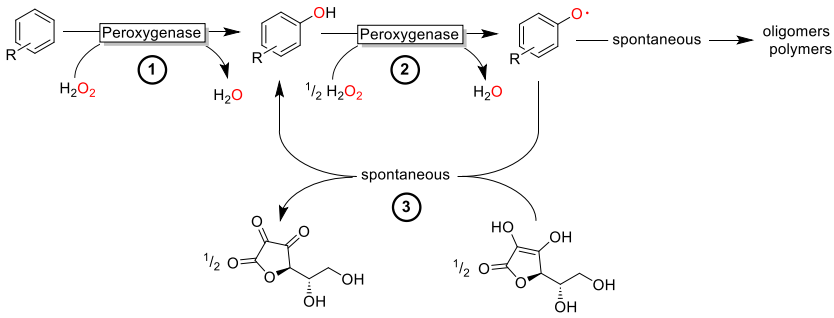

Fig. 4 Peroxygenase-catalysed arene hydroxylation. Step 1 represents the desired peroxygenase activity, which however often is coupled to the (undesired) peroxidase activity (step 2). The resulting radicals are prone to spontaneous radical polymerisation, which can be avoided by re-reduction of the phenoxy radical e.g. with ascorbate (step 3).

6. Protocols

6.1 Preparation of *Aae*UPO PaDa-I (Tieves et al., 2019b)

6.1.1 Materials

Basal salts media composition: Phosphoric acid (85 %): 26.7 mL; Potassium sulphate: 18.2 g; Magnesium sulphate-7H_2O: 14.9 g; Calcium sulphate: 0.93 g; Potassium hydroxide: 4.13 g; Glycerol: 40.0 g; Water: To a final volume of 1 L.

Trace salts solution (PTM1): Copper sulphate (5H_2O): 6.0 g; Sodium iodide: 0.08 g; Manganese sulphate-H_2O: 3.0 g; Zinc chloride: 20.0 g; Ferrous sulphate-7H_2O: 65.0 g; Cobalt chloride: 0.5 g; Sodium molybdate-2H_2O: 0.2 g; Boric acid: 0.02 g; Biotin: 0.2 g; Sulphuric acid: 5.0 mL; Water: To a final volume of 1 L.

Fermentation vessel: A 10 L glass fermenter filled with 6 L of basal salts media was autoclaved, and the pH was adjusted to 5.0 using ammonium hydroxide (29.5 %). PTM1 trace salts (4.35 mL/L) and antifoam C emulsion (20 % v/v, 1.0 mL/L) were added.

Fermentation Process.

Pre-culture: Grown overnight in BMGY medium with 25 μg/mL of Zeocin at 140 rpm and 30 °C.

Inoculation: The fermenter was inoculated with 800 mL of *Pichia pastoris* pre-culture.

Temperature and Agitation: The fermentation was carried out at 30 °C with constant agitation at 600 rpm and 5 L/min airflow.

Feeding Strategy: (1) Glycerol feeding phase: After the initial glycerol batch phase (lasting about 28 h), the glycerol feed was started. A 50 % glycerol solution (containing 12 mL/L PTM1 trace salts) was fed at a rate of 22–25 g/h keeping the dissolved oxygen (DO) concentration above 20 %.

(2) Methanol feeding phase: After 48 h, the glycerol feed was stopped, and 0.5 % (v/v) methanol was added to switch to methanol as carbon source and induce expression of *Aae*UPO. The methanol feed rate was adjusted between 5–17 g/h to maintain the DO level at around 30 %.

By the end of the fermentation, a cell wet weight of 165 g/L was achieved, and the final *Aae*UPO activity reached 172 ± 7 U/mL with a total activity of approximately 1,350,000 U in the bioreactor.

Notes: Oxygen is required for the first step of the methanol catabolism. Maintaining the DO during the methanol feeding phase above 20 % is important to ensure growth on methanol and reach high level of *Aae*UPO but may be difficult depending on the oxygen transfer rates of the fermenter used. To keep the DO above 20 %, 0.1–0.3 liter of O_2 per liter culture volume per min (vvm) is needed. At a constant airflow of 5 L/min, good growth and maximum expression levels were accomplished by gradually increasing the feeding rate by 5 % of the actual feeding rate when DO reached >35 % and reducing it by 5 % when DO reached <25 %.

6.2 Purification of *Aae*UPO

Clarification: After the fermentation, the culture broth was clarified via centrifugation to remove cell debris.

Concentration and Buffer Exchange: The supernatant was concentrated and the buffer was exchanged to 20 mM Tris/HCl (pH 7.0) using ultrafiltration. This yielded 304 mL of crude *Aae*UPO.

Anion Exchange Chromatography: Further purification was achieved using a Q Sepharose FF anion exchange column. After equilibration and an isocratic column wash, proteins were eluted using a linear gradient of NaCl (from 0.02 M to 0.2 M) in Tris/HCl buffer (20 mM, pH 7.0).

Desalting: Fractions containing *Aae*UPO were pooled and desalted using HiTrap Desalting columns.

Storage: The purified enzyme was stored at −20 °C.

6.3 Enzyme activity and concentration determination

Activity: *Aae*UPO activity was measured via an ABTS assay at 25 °C. The assay involved monitoring the oxidation of ABTS at 420 nm in a sodium citrate buffer (50 mM, pH 4.4) with 2 mM H_2O_2.

Concentration: The enzyme concentration was determined using its molar extinction coefficient at 420 nm ($\varepsilon = 115\ mM^{-1}\ cm^{-1}$). Additional methods, like CO difference spectra, were used for more precise concentration determination in non-purified samples.

CO difference spectra were recorded at 25 °C using Tris/HCl buffer (20 mM, pH 7.0) and sodium dithionite (50 mM). Samples were bubbled with CO for 60 s. The CO difference spectrum was recorded between 400 nm and 500 nm. The concentration was determined by absorbance difference between 445 nm and 490 nm ($\varepsilon = 107\ mM^{-1}\ cm^{-1}$).

6.4 Preparative-scale hydroxylation of cyclohexane to a mixture of cyclohexanol and cyclohexanone (Hilberath et al., 2023)

6.4.1 Materials used

Enzyme: lyophilised *Aae*UPO (PaDa-I variant) from *Agrocybe aegerita*.

Reaction Volume: 11 L in a 35 L jacketed glass reactor.

Solvent: 50 % (v/v) acetonitrile (ACN) in 100 mM potassium phosphate buffer at pH 6.

Substrate: Cyclohexane (600 mL) was the substrate at an initial concentration of 500 mM.

Oxidant: H_2O_2 as 12.75 M stock solution.

Analytics: GC-FID (Achiral CP-Wax 52 GB column), Quantofix peroxide 100 test strips.

6.5 Procedure

Enzyme Addition: 260 g of lyophilised *Aae*UPO (containing approximately 450 µmol of enzyme) was dissolved in 5 L of buffer and added into the reactor. UPO-concentrations from rehydrated concentrated supernatants are previously determined via CO-difference spectra using the extinction coefficient at 445 nm of $\varepsilon_{445} = 107\ mM^{-1}\ cm^{-1}$ (Tieves et al., 2019b). The final UPO-concentration should be 20 µM.

Substrate and Solvent Addition: 5.5 L of acetonitrile and cyclohexane were pumped into the reactor at a flow rate of 0.5 L/min. The mixing speed was set to 225 rpm. **Reaction Initiation:** The reaction was initiated by pumping the H_2O_2 solution at 120 mL/h, which sustained the

oxidation process. The reaction was monitored over 4 h. **Monitoring:** 5 mL samples are taken every 15 min to measure H_2O_2 levels via Quantofix peroxide test strips and a photometric H_2O_2 quantification assay such as the Pierce quantitative peroxide assay kit (Thermo Scientific Pierce, Rockford, IL, USA). Every hour, samples were extracted with ethylacetate and prepared for GC-FID analysis to quantify the products cyclohexanol and cyclohexanone.

6.6 Notes: Maximising *Aae*UPO robustness

The inactivation of *Aae*UPO represents a major issue for the robustness of the process. Therefore, making H_2O_2 the overall rate-limiting substrate is highly recommended. As the 'optimal' H_2O_2 addition rate depends on the reaction conditions (substrate, substrate concentration, enzyme concentration, (co-)solvents etc.) individual optimisation is necessary. We recommend starting with a H_2O_2-feed rate to less than 50 % of the expected maximal conversion rate (CR):

$$CR\,[mMh^{-1}] = 3600 \times k_{cat}\,[s^{-1}] \times c\,(\mathrm{Aae}UPO)\,[mM]$$

e.g. Cyclohexane-hydroxylation: $k_{cat} = 72\ s^{-1}$ (Peter et al., 2014).

The reagents are volatile, which is why mass balance issues are to be expected. We highly recommend NOT to base the analysis on relative GC-responses but to determine absolute concentrations based on calibration curves using internal standards.

6.7 *Aae*UPO-catalysed oxyfunctionalisation reactions using formate oxidase-catalysed *in situ* H_2O_2 generation (Tieves et al., 2019a; Willot et al., 2020)

Expression of *Ao*FOx: Expression System: Heterologous expression in *Escherichia coli* BL21 (DE3) using a pET21c(+) plasmid. **Culture Conditions:** The cells were cultured in Terrific Broth (TB) medium, supplemented with ampicillin (100 μg/mL). The main culture was inoculated to an OD600 of approximately 0.05 from the pre-culture and grown at 37 °C, 180 rpm. When the OD600 reached 0.6, IPTG (0.1 mM) was added to induce the expression of *Ao*FOx. Post-induction, the culture was incubated for an additional 6 h at 20 °C, 180 rpm.

Harvesting and Preparation: Harvesting: After the 6-hour induction, the cells were harvested by centrifugation and the cell pellets were washed and suspended in potassium phosphate buffer (50 mM, pH 7.5) containing PMSF (0.1 mM) to prevent proteolytic degradation. **Cell lysis:**

The cells were disrupted using a multi-shot cell disruption system to release the *Ao*FOx enzyme. **Clearing the lysate:** The lysate was clarified by centrifugation to obtain the supernatant containing the soluble formate oxidase enzyme.

Purification of *Ao*FOx: Affinity chromatography: The supernatant was applied to a HisTrap FF column for purification using a Biorad NGC system. **Equilibration:** The column was equilibrated with potassium phosphate buffer A (50 mM, pH 7.5, 0.5 M NaCl). **Elution:** A three-step gradient of potassium phosphate buffer B (50 mM, pH 8.3, 0.5 M NaCl, 0.5 M imidazole) was used for elution: 5 % buffer B, 27 % buffer B, 36 % buffer B.

Concentration and Desalting: The fractions containing *Ao*FOx were pooled and concentrated using Amicon filters (30 kDa cut-off). The enzyme was desalted with HiTrap Desalting columns using potassium phosphate buffer (25 mM, pH 7.5).

Analysis: Protein Concentration: The protein concentration of *Ao*FOx was determined by a **BCA assay**, with a result of 17.3 ± 0.8 mg/mL. **Purity:** The purity of *Ao*FOx was determined to be 67.6 % using SDS-PAGE. **Enzyme Activity:** *Ao*FOx activity was measured using an ABTS-assay with horseradish peroxidase. The assay was performed in acetate buffer (50 mM, pH 4.5) with ABTS (1 mM), HRP (10 U), and sodium formate (100 mM). The change in absorbance was followed at 420 nm. The specific activity of the preparation was 94.7 U/mg and the volumetric activity was 1642 ± 26 U/mL.

6.7.1 Semi-preparative hydroxylation of ethyl benzene

Reaction Setup: The reaction was carried out in 80 mL potassium phosphate buffer (100 mM, pH 6.0). **Substrate:** Ethylbenzene (5 mL, equivalent to 100 mM concentration). **Enzymes**: *Aae*UPO: 1.6 μM, *Ao*FOx: 166 nM. **Co-substrate:** Sodium formate (200 mM). **pH Control:** A pH STAT titration system (Metrohm) was used to maintain pH 6.0 throughout the reaction. Sulphuric acid (1 M) containing sodium formate (200 mM) was titrated to maintain the pH.

Product Isolation: The reaction mixture was extracted with ethyl acetate. The organic phase was concentrated to obtain the final product. The total amount of *(R)*-1-phenylethanol obtained was 434 mg, with approximately 13 % of the byproduct acetophenone. The purity of the *(R)*-1-phenylethanol was determined by ^{1}H NMR to be 97.5 % enantiomeric excess (ee).

6.8 Aromatic hydroxylation and counteracting radical polymerisation with ascorbate (Brasselet et al., 2024)

6.8.1 Fed-batch fermentation of Pichia pastoris X-33::pPICZA_AbrUPO

A fed-batch fermentation of *P. pastoris* X-33::pPICZA_*Abr*UPO was carried out in a 7.5 L bioreactor (Infors, Bottmingen, Switzerland) containing 3 L of basal salt medium supplemented with trace elements and biotin. The culture was inoculated to an OD600 of 0.5 from a preculture grown overnight in BMGY medium containing Zeocin™. The fermentation was maintained at pH 5.0, with the temperature initially set to 30 °C, while stirring at 800 rpm and supplying 3 L/min oxygen.

Upon glycerol depletion, 0.5 % (v/v) methanol containing 12 g/L PTM1 solution was introduced as a carbon source and inducer for gene expression. The temperature was reduced to 25 °C, and 10 μM hemin was added for efficient loading of *Abr*UPO. Automated methanol feeding was regulated by dissolved oxygen spikes. After 9 days of fermentation, cells were harvested by centrifugation. Volumetric activity towards ABTS, OD600, and protein concentration were measured at various time points during the fermentation process.

6.8.2 Biotransformation protocol

1. **Materials and Reagents:**
   - ***Abr*UPO:**
   - **Sodium ascorbate:** (50 mM final concentration, 5 equivalent excess to substrate).
   - **Phenolic substrate:** (e.g., trimethylphenol, 10 mM).
   - **H_2O_2:** Prepared freshly from a commercial 30 % (v/v) solution.
   - **Potassium phosphate buffer (KPi):** 100 mM, pH 6.0.
   - **Acetonitrile:** Solvent (10–15 % (v/v) in reaction buffer).
   - **GC-FID system:** For product analysis.
2. **Reaction Setup:**
   - **Buffer Preparation:** Dissolve potassium phosphate buffer to a final concentration of 100 mM, adjust pH to 6.0.
   - **Prepare Substrate Solution:** Dissolve the phenolic substrate in acetonitrile, diluting it to a final concentration of 10 mM in the buffer solution. The acetonitrile content should be between 10 and 15 vol%. The substrate has a low solubility in aqueous systems and should not crystallise in the reaction mixture.
   - **Enzyme Addition:** Add *Abr*UPO enzyme to the solution at a concentration of 0.8–4.1 μM.

- **Radical Scavenger Addition:** Add sodium ascorbate at a final concentration of 50 mM to the reaction mixture.
- **Hydrogen Peroxide Dosing:** Initiate the reaction by adding hydrogen peroxide to the mixture at a controlled rate of 5 mM/h. Continuous addition can be maintained using a syringe pump or manual titration. Ensure that the reaction mixture is well-agitated at 600 rpm during H_2O_2 addition.
- **Reaction Conditions: Temperature:** Maintain the reaction at 25 °C using a Eppendorf thermoshaker. **Reaction Time**: Maximum product concentrations are typically obtained after 5 h, with regular sampling for product analysis.
- **Sampling and Product Analysis: Sampling:** Take aliquots at 1-hour intervals to monitor the reaction progress. Quench samples by addition and shaking with ethyl acetate. **GC-FID Analysis:** Analyse samples using gas chromatography (GC) equipped with a flame ionisation detector (FID). Use *n*-dodecane as an internal standard and quantify substrates and products with calibration curves made priorly with authentic standards.

NOTES: Due to the peroxidase activity of *Abr*UPO towards substrate and products producing multimeric polymerisation products, reagent concentrations need to be based on calibration curves with authentic standards prepared under the same conditions the reaction is performed. Hydroquinones are O_2-labile compounds especially when no radical scavenger is present. Thus, storage and handling after product isolation should be handled under N_2-atomsphere.

6.9 Immobilisation of peroxygenase and application under non-aqueous conditions (Wang et al., 2023)

6.9.1 Enzyme immobilisation

Materials:

- ***Aae*UPO** (80 μM stock solution)
- **Amino resin** (LXTE-700): 1 g
- **Phosphate buffer** (pH 8.0, 50 mM)
- **Glutaraldehyde** (8 % v/v aqueous solution)
- **Thermal shaker** (set at 25 °C)
- **Centrifuge**

Protocol: 1. Preparation of Amino-Resin: Wash 1 g of the LXTE-700 resin three times with 50 mM phosphate buffer (pH 8.0). Filter the resin

and set aside. **2. Activation of Resin:** Add 320 μL of 8 % glutaraldehyde to the washed resin along with 3.68 mL of phosphate buffer. Incubate the mixture on a thermal shaker at 22 °C, 220 rpm for 1 h. Wash the resin three more times with phosphate buffer to remove excess glutaraldehyde. **3. Enzyme Immobilisation:** Add 400 μL of the UPO solution (8 μM) to the activated resin along with 3.6 mL of phosphate buffer. Shake the mixture on the thermal shaker at 25 °C for 3 h. After incubation, remove the supernatant and wash the resin three times with phosphate buffer. **Storage:** The wet pellet of immobilised *Aae*UPO (can be used directly for catalysis or stored at 4 °C for short-term use). **Enzyme Loading Efficiency:** Measure the enzyme concentration before and after immobilisation by recording UV-Vis absorbance at 420 nm. Calculate the binding efficiency. Typically, the binding efficiency of *Aae*UPO on the resin is 37.5 %, corresponding to an enzyme loading of 12 nmol/g of resin.

6.10 Biotransformation

6.10.1 Materials

- **Immobilised *Aae*UPO** (prepared as described above)
- **Substrate (e.g., thioether)**
- **tert-Butyl hydroperoxide (tBuOOH) in decane (5.0 M)**
- **Decane**: Organic solvent
- **Phosphate buffer (50 mM, pH 8.0)**
- **Thermal shaker**
- **Syringe pump**

Protocol: 1. Reaction Setup: Add 100–400 mg of immobilised *Aae*UPO to a glass vial. Introduce 0.5 mL of the substrate (neat) into the vial. Prepare a solution of tBuOOH in decane (1.5 M) and set up a syringe pump to deliver the solution at a rate of 6–15 mM/h (equivalent to 5 μL/h relative to the reaction volume). Incubate the reaction mixture in a thermal shaker at 30 °C, 800 rpm. Maintain the reaction for 0–72 h depending on the desired level of conversion. **Monitoring Reaction Progress:** At regular intervals, withdraw aliquots and analyze the reaction mixture via GC or HPLC to determine conversion rates and enantiomeric excess (ee) of the products. **Reaction Termination and Product Isolation:** At the end of the reaction, filter the mixture to remove the immobilised enzyme. Extract the organic phase (containing the product) with dichloromethane (DCM) and dry the organic layer over sodium sulphate (Na_2SO_4). Concentrate the organic phase under reduced pressure and purify the product using silica column chromatography.

References

Anderson, S. R., Bommarius, B. R., Woodley, J. M., & Bommarius, A. S. (2021). Sparged but not stirred: Rapid, ADH-NADH oxidase catalyzed deracemization of alcohols in a bubble column. *Chemical Engineering Journal, 417*, 127909.

Beltrán-Nogal, A., Sánchez-Moreno, I., Méndez-Sánchez, D., Gómez De Santos, P., Hollmann, F., & Alcalde, M. (2022). Surfing the wave of oxyfunctionalization chemistry by engineering fungal unspecific peroxygenases. *Current Opinion in Structural Biology, 73*, 102342.

Birmingham, W. R., Toftgaard Pedersen, A., Dias Gomes, M., Bøje Madsen, M., Breuer, M., Woodley, J. M., & Turner, N. J. (2021). Toward scalable biocatalytic conversion of 5-hydroxymethylfurfural by galactose oxidase using coordinated reaction and enzyme engineering. *Nature Communications, 12*(1), 4946.

Brasselet, H., Schmitz, F., Koschorreck, K., Urlacher, V. B., Hollmann, F., & Hilberath, T. (2024). Selective peroxygenase-catalysed oxidation of phenols to hydroquinones. *Advanced Synthesis & Catalysis, 366*(21), 4430–4435.

But, A., van Noord, A., Poletto, F., Sanders, J. P. M., Franssen, M. C. R., & Scott, E. L. (2017). Enzymatic halogenation and oxidation using an alcohol oxidase-vanadium chloroperoxidase cascade. *Molecular Catalysis, 443*, 92–100.

Dias Gomes, M., Bommarius, B. R., Anderson, S. R., Feske, B. D., Woodley, J. M., & Bommarius, A. S. (2019). Bubble column enables higher reaction rate for deracemization of (R,S)-1-phenylethanol with coupled alcohol dehydrogenase/NADH oxidase system. *Advanced Synthesis & Catalysis, 361*(11), 2574–2581.

Dordick, J. S., Marletta, M. A., & Klibanov, A. M. (1987). Polymerization of phenols catalyzed by peroxidase in nonaqueous media. *Biotechnology and Bioengineering, 30*(1), 31–36.

Dordick, J. S., Marletta, M. A., & Klibanov, A. M. (1986). Peroxidase depolymerize lignin in organic media but not in water. *Proceedings of the National Academy of Sciences of the United States of America, 83*(17), 6255–6257.

Gomez de Santos, P., Mateljak, I., Hoang, M. D., Fleishman, S. J., Hollmann, F., & Alcalde, M. (2023). Repertoire of computationally designed peroxygenases for enantiodivergent C–H oxyfunctionalization reactions. *Journal of the American Chemical Society, 145*, 3443–3453.

Hilberath, T., Van Oosten, R., Victoria, J., Brasselet, H., Alcalde, M., Woodley, J. M., & Hollmann, F. (2023). Toward kilogram-scale peroxygenase-catalyzed oxyfunctionalization of cyclohexane. *Organic Process Research & Development, 27*(7), 1384–1389.

Hilberath, T., Van Troost, A., Alcalde, M., & Hollmann, F. (2022). Assessing peroxygenase-mediated oxidations in the presence of high concentrations of water-miscible co-solvents. *Frontiers in Catalysis, 2*, 882992.

Hobisch, M., Holtmann, D., De Santos, P. G., Alcalde, M., Hollmann, F., & Kara, S. (2021). Recent developments in the use of peroxygenases – Exploring their high potential in selective oxyfunctionalisations. *Biotechnology Advances, 51*, 107615.

Hrycay, E. G., Gustafsson, J. A., Ingelmansundberg, M., & Ernster, L. (1975). Sodium periodate, sodium-chlorite, organic hydroperoxides, and H_2O_2 as hydroxylating agents in steroid hydroxylation reactions catalyzed by partially purified cytochrome-P-450. *Biochemical and Biophysical Research Communications, 66*(1), 209–216.

Karich, A., Scheibner, K., Ullrich, R., & Hofrichter, M. (2016). Exploring the catalase activity of unspecific peroxygenases and the mechanism of peroxide-dependent heme destruction. *Journal of Molecular Catalysis B: Enzymatic, 134*, 238–246.

Lindeque, R. M., & Woodley, J. M. (2020). The effect of dissolved oxygen on kinetics during continuous biocatalytic oxidations. *Organic Process Research and Development, 24*(10), 2055–2063.

Molina-Espeja, P., De Santos, P. G., & Alcalde, M. (2017). Directed evolution of unspecific peroxygenase. In M. Alcalde (Ed.). *Directed enzyme evolution: Advances and applications* (pp. 127–143). Cham: Springer International Publishing.

Molina-Espeja, P., Garcia-Ruiz, E., Gonzalez-Perez, D., Ullrich, R., Hofrichter, M., & Alcalde, M. (2014). Directed evolution of unspecific peroxygenase from *Agrocybe aegerita*. *Applied and Environmental Microbiology, 80*(11), 3496–3507.

Molina-Espeja, P., Ma, S., Mate, D. M., Ludwig, R., & Alcalde, M. (2015). Tandem-yeast expression system for engineering and producing unspecific peroxygenase. *Enzyme and Microbial Technology, 73–74*(0), 29–33.

Monterrey, D. T., Menés-Rubio, A., Keser, M., Gonzalez-Perez, D., & Alcalde, M. (2023). Unspecific peroxygenases: The pot of gold at the end of the oxyfunctionalization rainbow? *Current Opinion in Green and Sustainable Chemistry, 41*, 100786.

Morris, D. R., & Hager, L. P. (1966). Chloroperoxidase.I. Isolation and properties of crystalline glycoprotein. *The Journal of Biological Chemistry, 241*(8), 1763–1768.

Münch, J., Dietz, N., Barber-Zucker, S., Seifert, F., Matschi, S., Püllmann, P., & Weissenborn, M. J. (2024). Functionally diverse peroxygenases by alphaFold2, design, and signal peptide shuffling. *ACS Catalysis, 14*(7), 4738–4748.

Münch, J., Soler, J., Hünecke, N., Homann, D., Garcia-Borràs, M., & Weissenborn, M. J. (2023). Computational-aided engineering of a selective unspecific peroxygenase toward enantiodivergent β-ionone hydroxylation. *ACS Catalysis, 13*(13), 8963–8972.

Peter, S., Karich, A., Ullrich, R., Grobe, G., Scheibner, K., & Hofrichter, M. (2014). Enzymatic one-pot conversion of cyclohexane into cyclohexanone: Comparison of four fungal peroxygenases. *Journal of Molecular Catalysis B: Enzymatic, 103*, 47–51.

van Rantwijk, F., & Sheldon, R. A. (2000). Selective oxygen transfer catalysed by heme peroxidases: Synthetic and mechanistic aspects. *Current Opinion in Biotechnology, 11*(6), 554–564.

De Santos, P. G., González-Benjumea, A., Fernandez-Garcia, A., Aranda, C., Wu, Y., But, A., ... Alcalde, M. (2023). Engineering a highly regioselective fungal peroxygenase for the synthesis of hydroxy fatty acids. *Angewandte Chemie International Edition, 62*, e202217372.

Sayoga, G. V., Bueschler, V. S., Beisch, H., Utesch, T., Holtmann, D., Fiedler, B., & Liese, A. (2023). Electrochemical H_2O_2 – Stat mode as reaction concept to improve the process performance of an unspecific peroxygenase. *New Biotechnology, 78*, 95–104.

Van Schie, M., Spöring, J.-D., Bocola, M., Dominguez de Maria, P., & Rother, D. (2021). Applied biocatalysis beyond just buffers – From aqueous to unconventional media. Options and guidelines. *Green Chemistry: An International Journal and Green Chemistry Resource: GC, 23*, 3191–3206.

Shen, Q., Yan, J., Han, Y., Zhang, Z., Li, H., Kong, D., & Zhang, W. (2024). Peroxygenase-enabled reductive kinetic resolution for the enantioenrichment of organoperoxides. *Angewandte Chemie International Edition, 63*, e202401590.

Tieves, F., Tonin, F., Fernández-Fueyo, E., Robbins, J. M., Bommarius, B., Bommarius, A. S., ... Hollmann, F. (2019b). Energising the E-factor: The E^+-factor. *Tetrahedron, 75*, 1311–1314.

Tieves, F., Willot, S. J.-P., van Schie, M. M. C. H., Rauch, M. C. R., Younes, S. H. H., Zhang, W., ... Hollmann, F. (2019a). Formate oxidase (FOx) from *Aspergillus oryzae*: One catalyst to promote H_2O_2-dependent biocatalytic oxidation reactions. *Angewandte Chemie International Edition, 58*, 7873–7877.

Ullrich, R., Nüske, J., Scheibner, K., Spantzel, J., & Hofrichter, M. (2004). Novel haloperoxidase from the agaric basidiomycete *Agrocybe aegerita* oxidizes aryl alcohols and aldehydes. *Applied and Environmental Microbiology, 70*(8), 4575–4581.

Van De Velde, F., Lourenço, N. D., Bakker, M., van Rantwijk, F., & Sheldon, R. A. (2000). Improved operational stability of peroxidases by coimmobilization with glucose oxidase. *Biotechnology and Bioengineering, 69*(3), 286–291.

Wang, Y., Teetz, N., Holtmann, D., Alcalde, M., van Hengst, J. M. A., Liu, X., & Hollmann, F. (2023). Selective peroxygenase-catalysed oxidation of toluene derivates to benzaldehydes. *ChemCatChem, 15*, e202300645.

Willot, S. J. P., Hoang, M. D., Paul, C. E., Alcalde, M., Arends, I., Bommarius, A. S., & Hollmann, F. (2020). FOx news: Towards methanol-driven biocatalytic oxyfunctionalisation reactions. *ChemCatChem, 12*, 2713–2716.

Wu, Y., Paul, C. E., & Hollmann, F. (2024). Mirror, mirror on the wall, which is the greenest of them all? A critical comparison of chemo- and biocatalytic oxyfunctionalisation reactions. *Green Carbon, 1*(2), 227–241.

Zaks, A., & Klibanov, A. M. (1985). Enzyme-catalyzed processes in organic-solvents. *Proceedings of the National Academy of Sciences of the United States of America, 82*(10), 3192–3196.

Zaks, A., & Klibanov, A. M. (1984). Enzymatic catalysis in organic media at 100-degrees-C. *Science (New York, N. Y.), 224*(4654), 1249–1251.

Zhang, W., Fernández-Fueyo, E., Ni, Y., van Schie, M., Gacs, J., Renirie, R., & Hollmann, F. (2018). Selective aerobic oxidation reactions using a combination of photocatalytic water oxidation and enzymatic oxyfunctionalizations. *Nature Catalysis, 1*, 55–62.